Hierarchical Self-Assembly of Supramolecular Spintronic Modules into 1D- and 2D-Architectures with Emergence of Magnetic Properties

Mario Ruben,[a, b] Ulrich Ziener,[a, c] Jean-Marie Lehn,*[a] Vadim Ksenofontov,[d] Philipp Gütlich,*[d] and Gavin B. M. Vaughan[e]

Abstract: Hierarchical self-assembly of complex supramolecular architectures allows for the emergence of novel properties at each level of complexity. The reaction of the ligand components **A** and **B** with Fe^{II} cations generates the [2×2] grid-type functional building modules **1** and **2**, presenting spin-transition properties and preorganizing an array of coordination sites that sets the stage for a second assembly step. Indeed, binding of La^{III} ions to **1** and

Keywords: functional emergence · metallosupramolecular grids · self-assembly · spin transition · supramolecular chemistry

of Ag^{I} ions to **2** leads to a 1D columnar superstructure **3** and to a wall-like 2D layer **4**, respectively, with concomitant modulation of the magnetic properties of **1** and **2**. Thus, to each of the two levels of structural complexity generated by the two sequential self-assembly steps corresponds the emergence of novel functional features.

Introduction

A major present thrust in supramolecular chemistry concerns the processes underlying self-organization, the goals being to understand their origin and operation, to induce the emergence of novel properties at each level of complexity, and to achieve their implementation in artificial functional systems.[1]

[a] Dr. M. Ruben, Dr. U. Ziener, Prof. Dr. J.-M. Lehn
ISIS
8 Allée Gaspard Monge
67000 Strasbourg (France)
Fax: (+33) 03-90-24-51-40
E-mail: lehn@isis.u-strasbg.fr

[b] Dr. M. Ruben
Current address: Institute of Nanotechnology
Research Center Karlsruhe, PF 3640
76021 Karlsruhe (Germany)

[c] Dr. U. Ziener
Current address: Organische Chemie III
Makromolekulare Chemie University of Ulm
Albert Einstein Allee 11
89069 Ulm (Germany)

[d] Dr. V. Ksenofontov, Prof. Dr. P. Gütlich
Institut für Anorganische Chemie und Analytische Chemie
Johannes Gutenberg-Universität Mainz
Staudingerweg 9, 55099 Mainz (Germany)

[e] Dr. G. B. M. Vaughan
European Synchrotron Radiation Facility (ESRF)
Beamline 11, BP 220
38043 Grenoble Cedex (France)

The generation of organization levels of increasing complexity, diversity and functionality relies on a set of basic building blocks and subunits, interconnected through a multitude of relatively weak, non-covalent interactions (e.g. hydrogen, van der Waals and coordinative bonding, etc.).[1,2] It rests on the progressive build-up of more and more complex entities by multiple, sequential and hierarchical self-organization steps, following a conditional pathway, each step setting the base for the next one. Hierarchical self-organization[3,4] may be driven by more or less pronounced positive cooperativity, up to a phase change, such as the formation of a liquid crystalline or a solid state.

In recent years, more and more powerful self-assembly strategies have been developed for the controlled access to a variety of nano-sized objects of increasing complexity. Much work was addressed to the understanding and manipulation of the parameters which give access to a variety of nano-architectures, in particular of metallo-supramolecular type, such as rods, squares, circles, cages, clamps, emphasizing mainly structural aspects like size, symmetry and chirality of the products.[5] Less attention has been paid to self-assembled architectures exhibiting discrete functional properties (switching, moving etc.).[6]

Such functional architectures may derive from three principal routes: i) the functionality may result as "emerging" property from the assembly of the building modules; ii) the functionality may be encoded on the isolated modules and persist as unchanged property in the self-assembled architecture or iii) the two approaches above may also partially

merge, since the molecular surroundings can alter or tune an original, "module-based", functionality to a large extent and lead to the gradual appearance of new functional features.[7–9]

Herein, we report on the hierarchical self-assembly of the magnetic molecular architectures **3** and **4**. It involves in a first step the assembly of the ligand components **A** and **B** and Fe^{II} ions into the supramolecular spintronic modules[9b] **1** and **2**, displaying magnetic properties based on the spin-transition phenomenon and preorganizing an array of binding sites that sets the stage for a second step. This newly gained "collective" property is modulated through a subsequent, higher order self-assembly process induced by binding of a new set of cations and generating the 1D and 2D architectures **3** and **4**, respectively. The structural and magnetic properties of the four architectures **1**–**4** were investigated in detail at the two hierarchical organisation levels.

Results and Discussion

Synthesis and structures of the [2×2] grid-type complexes [Fe$^{II}_4$L$_4$]$^{8+}$, 1 and 2: It has been shown that tetranuclear molecular systems of the [2×2] grid type with four precisely located transition metal ions are accessible by self-organisation and exhibit interesting electrochemical, magnetic and optical properties.[8, 9] The nature of the substitutions of the ligand can induce for M^{II} = Fe the occurrence of spin transition in the [Fe$^{II}_4$L$_4$]$^{8+}$ units.[9]

We designed ligand components **A** and **B**, which should be able to undergo two hierarchical self-assembly steps through the stepwise coordination of different metal ions, such as Fe^{II} and La^{III} (for **A**) or Fe^{II} and Ag^{I} (for **B**), generating first the respective [2×2]Fe$_4$ grids, as building modules, and interconnecting thereafter these units via coordination of a second type of metal ion. In a earlier study, a related ligand contained sites for a second assembly step through hydrogen bonding.[10] The synthesis and first results of the coordination behaviour of the ligands **A** and **B** were reported earlier.[11]

Abstract in French: *L'autoassemblage hiérarchisé d'architectures supramoléculaires conduit à l'émergence de nouvelles propriétés à chaque niveau de complexité. La réaction des ligands A et B avec des cations Fe^{II} génère des modules fonctionnels de type grille [2×2], 1 et 2, qui présentent des propriétés de transition de spin, et prédisposent un ensemble de sites de coordination pour une deuxième étape d'assemblage. En effet, la complexation d'ions La^{III} par 1 et d'ions Ag^{I} par 2 conduit respectivement à une superstructure colonnaire 3 1D et à un arrangement en feuillet 2D, avec une modulation concomitante des propriétés magnétiques de 1 et 2. Ainsi, à chaque niveau de complexité structurale généré par les deux étapes d'autoassemblage séquentiel, correspond l'émergence de nouvelles propriétés fonctionnelles.*
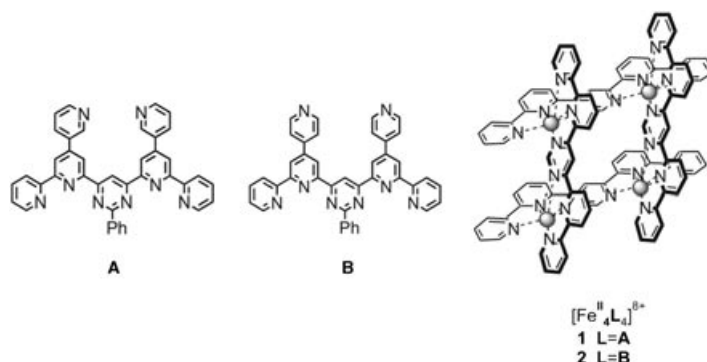
The compounds, [Fe$_4$**A**$_4$](BF$_4$)$_8$ (**1**) and [Fe$^{II}_4$**B**$_4$](BF$_4$)$_8$ (**2**), were obtained by assembly from the corresponding ligand **A** or **B** and [Fe(BF$_4$)$_2$]×6H$_2$O in acetonitrile at reflux for eight hours, followed by precipitation with diisopropyl ether (Figure 1). The composition of **1** and **2** was confirmed by FAB-mass spectrometry and elemental analysis. No evidence for higher-mass polymeric products was found in ES-mass spectrometry investigations.

The ^{1}H NMR spectra of **1** and **2** at 298 K both exhibit fourteen singlets covering a range from $\delta = -10$ to 150 ppm. The number of signals is indicative of C_{2v} symmetry of the coordinated ligands **A** or **B** and of a hindered rotation of the phenyl groups with free rotation of the pyridine units. The spread-out chemical shift domain covered by the signals results from paramagnetic contact shifts of Fe^{II}(HS) ions.[12]

The structure of [Fe$^{II}_4$**B**$_4$]$^{8+}$ (**2**) (as the perchlorate compound) was determined by single crystal X-ray diffraction at 120 K (Figure 2). It consists of a tetranuclear complex in which each of the Fe^{II} ions is in a pseudo-octahedral arrangement with a pronounced axial distortion. Each metal ion is surrounded by six nitrogen atoms from the pyrimidine and bipyridine groups. The Fe−N bond lengths of d(Fe−N) = 1.898(6)–2.103(6) Å indicate that at 120 K all four Fe^{II} ions are in their LS state.[9] A single chloride anion, coming presumably from impurities of the [Fe(ClO$_4$)$_2$]×6H$_2$O salt used, is bound in the central cavity of the [Fe$^{II}_4$**B**$_4$]$^{8+}$ cation, while the remaining seven ClO$_4$ anions are found together with solvent and water molecules in the crystal lattice around the complex cation.

The four ligands **B** are bound to the Fe^{II} ions by their terpyridine-type coordination sites formed from lateral four pyridine and the central pyrimidine groups, while the eight 4-pyridyl units point orthogonally above and below the main molecular plane containing the four metal ions. The central C–C axes connecting the terpy moieties with the *exo*-directed 4-pyridines deviate by 5.2 up to 29.5° from ideal orthogonality. As a consequence, all pyridine groups are slightly bent outside, and the free nitrogen atoms are easily accessible for further coordination.

The first self-assembly process incorporates the four ligands **B** in the complex [Fe$^{II}_4$**B**$_4$]$^{8+}$ (**2**) and, at the same time, pre-organizes them in a disposition which enables further
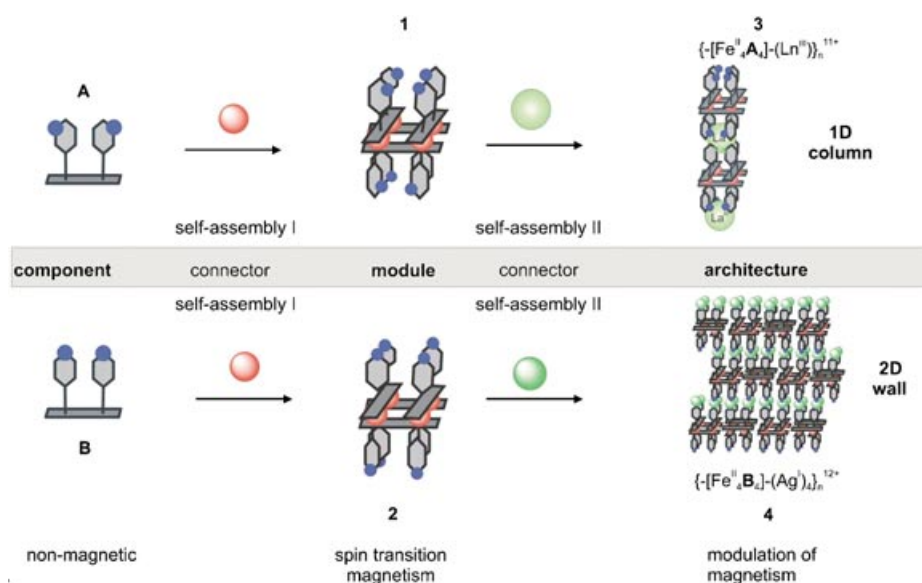
Figure 1. Two-step hierarchical self-assembly of metallosupramolecular architectures with emergence of magnetic properties. From ligands **A** and **B** to the magnetic [2×2] grid-type building modules $[Fe_4^{II}A_4]^{8+}$ (**1**) and $[Fe_4^{II}B_4]^{8+}$ (**2**) (self-assembly I), and on to the columnar 1-D architecture $\{[-Fe_4^{II}A_4]-(La^{III})_4\}_n^{11+}$ (**3**) and the wall-like 2-D architecture $\{[-Fe_4^{II}B_4]-(Ag^I)_4\}_n^{12+}$ (**4**) (self-assembly II). Red spheres: Fe^{II}, green spheres (top): La^{III}, green spheres (bottom) Ag^I. Bottom: emerging magnetic properties.
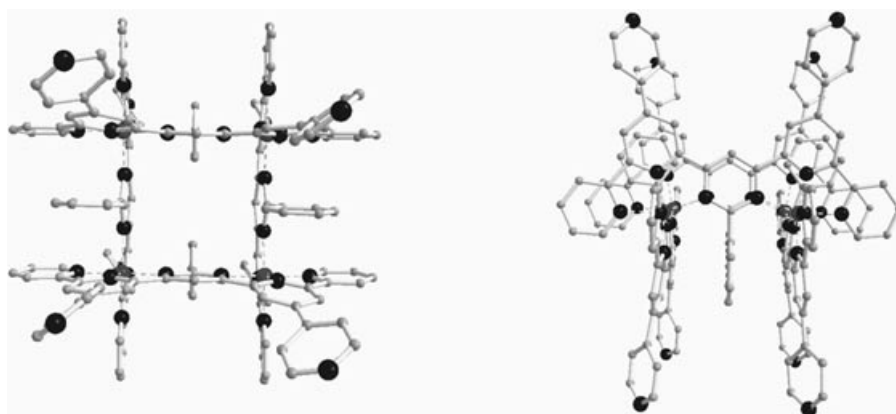
Figure 2. Top and side view of the [2×2] grid-type complex $[Fe_4^{II}B_4]^{8+}$ (**2**) in the crystal structure (anions, solvent molecules, hydrogen atoms and the rotational disorder of the pyridine groups are omitted for clarity).

metal ion coordination to the building module generated, for a higher order second self-assembly step.

The analytical data for the complex $[Fe_4^{II}A_4]^{8+}$ (**1**) are very similar to those obtained for complex **2** (see Experimental Section) and point to an identical composition.

Synthesis and structures of the extended coordination architectures $\{[Fe_4^{II}A_4]-(La^{III})_4\}_n^{11+}$ (3) and $\{[Fe_4^{II}B_4]-(Ag^I)_4\}_n^{12+}$ (4): The generation of a second order coordination assembly was achieved by connecting the tetranuclear grid modules $[Fe_4^{II}A_4]^{8+}$ (**1**) through binding of lanthanum(III) ions. The reaction was performed by layering an acetonitrile solution of **1** (as its ClO_4^- salt) with a six-fold excess of a $[La(ClO_4)_3]$ in methanol resulting in deep-green, triangular-shaped crystals of assembly **3**. Elemental analysis of these crystals point

to a $\{-[Fe_4^{II}A_4]-(La^{III})\}(ClO_4)_{11}$ composition with additional sixteen water and two acetonitrile molecules. Single crystal X-ray investigations reveal an one-dimensional columnar motif involving aligned alternating $[Fe_4^{II}(A)_4]^{8+}$ and coordinated La^{III} ions. The data reveal the tetranuclear Fe_4^{II} modules, interconnected in a linear fashion by the coordination of a La^{III} ion to two four-fold sets of 3-pyridyl groups above and below the Fe_4^{II} plane of two neighbouring modules. Unfortunately, due to the bad quality of the crystals and despite several attempts to improve the quality of the data, the resulting elevated *R* factor does not allow a more detailed discussion of the molecular structure of $\{[Fe_4^{II}A_4]-(La^{III})_4\}_n^{11+}$ (**3**). However, the overall motif described above is secure.

To achieve a second order assembly of module $[Fe_4^{II}B_4]^{8+}$ (**2**), a solution of its BF_4^- salt in acetonitrile was layered with a solution of methanol containing six equivalents of $AgBF_4$. After several weeks, pine-green prisms of compound **4** had grown at the diffusion interface of the two solutions. The overall composition of the compound was determined as $\{[Fe_4^{II}B_4]-(Ag^I)_4\}(BF_4)_{10}(SiF_6)$ by elemental analysis and its structure was determined by X-ray investigations of the crystalline material. The structure of the cationic $[Fe_4^{II}B_4]^{8+}$ subunits within **4** is of [2×2] grid type, very similar to that determined for **2** with Fe—N bond lengths of $d(Fe-N) = 1.890(7)–2.092(6)$ Å, indicating the presence of exclusively $Fe^{II}(LS)$ ions at 120 K. All eight *exo*-4-pyridyl groups of each $[Fe_4^{II}B_4]^{8+}$ unit were coordinated to Ag^I ions (Figures 1 and 3). Attempts to dissolve the complex in polar solvents (DMF, DMSO) resulted in the break-up of **4** into the tetranuclear $[Fe_4^{II}B_4]^{8+}$ units and solvated Ag^I ions.

The Ag^I ions are dicoordinated in an approximately linear coordination manner with $d(Ag-N) = 2.130(12)–2.228(14)$ Å; $\alpha(N-Ag-N) = 166.4(7)$ and $168.8(8)°$, and interconnect successive tetranuclear $[Fe_4^{II}B_4]^{8+}$ units through four pyridine–Ag^I–pyridine bridges. Following this coordination scheme, an infinite coordination polymer is generated
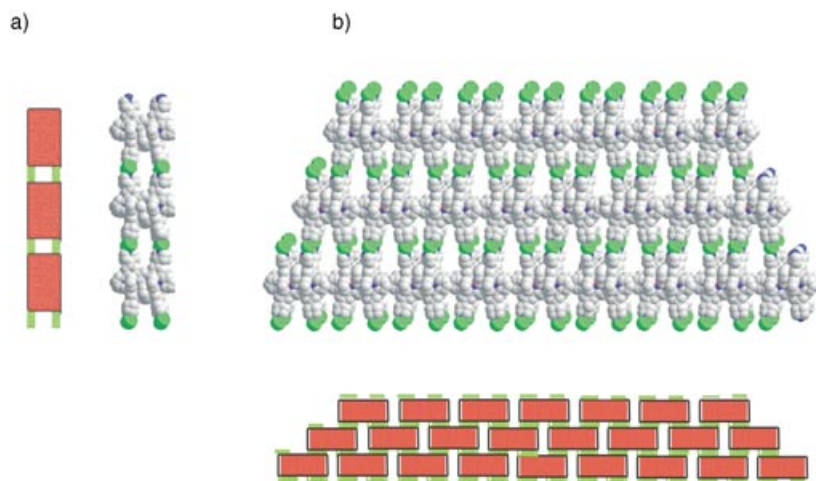
Figure 3. X-ray single crystal structure of $\{[Fe_4^{II}B_4]\text{-}(Ag^I)_4\}_n^{12+}$ (**4**) displaying the wall-like 2D interconnection of the $[Fe_4^{II}B_4]^{8+}$ [2×2] grid-type building modules (red) by the Ag^I ions (green): a) cross section; b) frontal elevation of the 2D wall-like array (anions and solvent molecules are omitted for clarity; carbon: grey, nitrogen: blue, iron: red).

as a meander-like interwoven, two-dimensional network (Figure 3). Within this wall-like array, the $[Fe_4^{II}B_4]^{8+}$ building modules are aligned in rows at 2.15 nm apart, while the distance between two neighbouring "walls" is about 1.56 nm. The central and peripheral cavities within the $[Fe_4^{II}B_4]^{8+}$ units, but not the hollow space around the Ag^I ions, are filled with the BF_4^- anions and solvent molecules (Figure 3).

Magnetic properties of the units 1 and 2 and of the assemblies 3 and 4: The magnetic properties of module $[Fe_4^{II}A_4](ClO_4)_8$ (**1**) and of the extended assembly $\{\text{-}[Fe_4^{II}A_4]\text{-}(La^{III})\}(ClO_4)_{(11)n}$ (**3**) are represented in Figure 4a as $\chi_M T/4$ versus T plots, χ_M being the molar magnetic susceptibility, corrected for diamagnetic contributions ($\chi_D = -357.8 \times 10^{-6}$ cm^3 mol^{-1}) using Pascal's constants, and T the temperature. At room temperature, $\chi_M T/4$ of **1** is equal to 3.2 cm^3 K mol^{-1}, close to the spin-only value expected for four high-spin Fe^{II} ions. On lowering the temperature, $\chi_M T/4$ progressively decreases reaching a value of 1.2 cm^3 K mol^{-1} at 30 K, calling for the presence of one to two HS Fe^{II} (a situation already found in other $[Fe_4^{II}L_4]^{8+}$ units).[9a] Below this temperature, $\chi_M T/4$ drops, which can be attributed to zero-field splitting of the Fe^{II}(HS) ions.[13] The very gradual increase and the absence of any hysteresis in the $\chi_M T/4$ versus T plot suggests that the cooperative interactions accompanying spin transition are rather weak. This was already observed for other members of this class of compounds and is apparently characteristic for the spin transition behaviour of these systems.[9,14] The magnetic properties of **1** (as well as of **2**, below) emerge from the assembly and are absent in the components, the ligands and metal ions.

Upon aligning the $[Fe_4^{II}A_4]^{8+}$ modules into the one-dimensional coordination polymer $\{\text{-}[Fe_4^{II}A_4]\text{-}(La^{III})\}_n(ClO_4)_{(11)n}$ (**3**), the unit-based spin transition behaviour persists, but the whole magnetic curve is shifted towards stabilization of the LS state (Figure 4a). At low temperature, below 50 K, a pla-

teau with almost no remaining magnetic moment and the absence of any Fe^{II}(HS)-based zero-field splitting indicates a completely diamagnetic situation only involving four Fe^{II}(LS) (each with S=0). At room temperature, a maximum value of 1.8 cm^3 K mol^{-1} evokes an incomplete spin transition in accordance with the shift of T_c to higher temperatures.

The magnetic properties of module $[Fe_4^{II}B_4](BF_4)_8$ (**2**) and its assembly $\{\text{-}[Fe_4^{II}B_4]\text{-}(Ag^I)_4\}_n(BF_4)_{(12)n}$ (**4**) are represented in Figure 4b. At room temperature, $\chi_M T/4$ for **2** is equal to 2.4 cm^3 K mol^{-1} and thus in the range of values expected for three HS and one LS
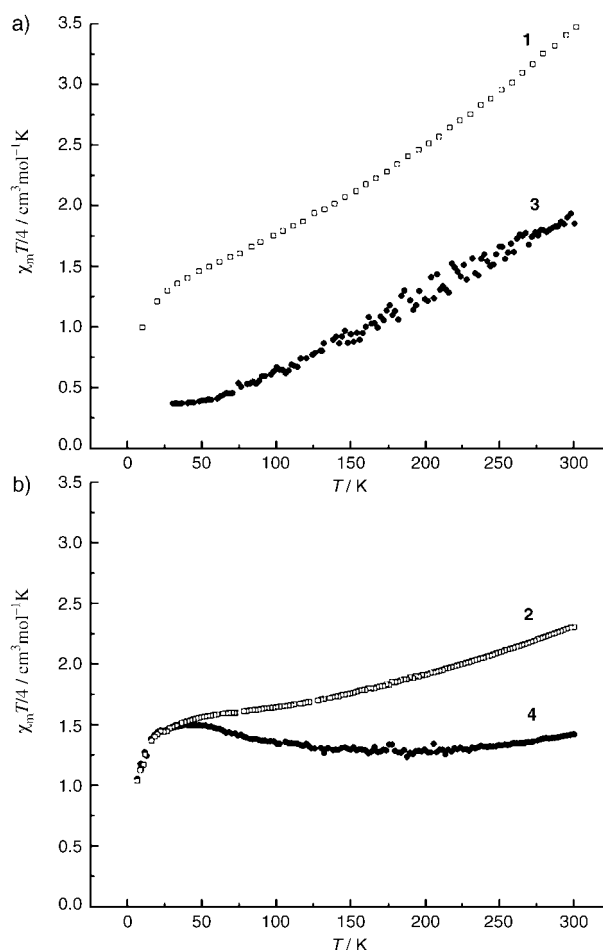
Figure 4. $\chi_M T/4$ versus temperature plots of a) the module $[Fe_4^{II}A_4](ClO_4)_8$ (**1**) and the columnar assembly $\{[Fe_4^{II}A_4]\text{-}(La^{III})\}(ClO_4)_{(11)n}$ (**3**); b) the module $[Fe_4^{II}B_4](BF_4)_8$ (**2**) and the wall-like assembly $\{\text{-}[Fe_4^{II}B_4]\text{-}(Ag^I)_4\}_n(BF_4)_{(12)n}$ (**4**).

Fe^{II} ions; it decreases on lowering the temperature reaching a value of $1.4 \, cm^3 \, K \, mol^{-1}$ at 30 K, calling for the presence of two Fe^{II}(HS). The magnetic data show a very gradual and, in comparison with **1**, a very incomplete spin transition process as already observed for other members of this class of compounds.[9]

The magnetic behaviour of the two-dimensional, wall-like assembly **4** $\{[Fe_4^{II}B_4]\text{-}(Ag^I)_4\}_n(BF_4)_{(12)n}$ is shown in Figure 4b. At room temperature, $\chi_M T/4$ of **4** is equal to $1.4 \, cm^3 \, K \, mol^{-1}$ which is significantly lower than found for the constituting complex **2** itself and points at a magnetic situation involving two Fe^{II}(LS) and two Fe^{II}(HS) ions. On lowering the temperature the magnetic moment of **4** remains almost unchanged before showing a slight increase to $\chi_M T/4 = 1.5 \, cm^3 \, K \, mol^{-1}$ at $T = 30$ K. Below that temperature, once more, a sharp drop due to the zero field splitting of Fe^{II}(HS) ions is observed.[13]

The spin transition in the assembly **4** is, in comparison with module **2**, inhibited over the whole temperature range studied, possibly due to steric hindrance in the interconnected, two-dimensional network. Since the conversion of Fe^{II}(LS) to Fe^{II}(HS) is accompanied by a volume increase, each spin transition would have to expand against the, more rigid, 2D network of **4**.[14,15] As a result, the magnetic moment remains close to the value of the non-bridged "monomer" **2** at low temperature (30 K). The observed slight decrease of the $\chi_M T$ versus T curve between 300 and 150 K may be due to weak antiferromagnetic intramolecular interaction as already observed in the analogous $[Co_4^{II}L_4]^{8+}$ compounds.[8b] The increase of χT below about 150 but above 30 K, might result from ferromagnetic intermolecular exchange coupling between the neighbouring 2D-networks (Figure 4b), although such coupling should be very weak over a distance of 15 Å.

Conclusion

The present results show that hierarchically ordered self-assembly processes using suitably designed molecular components can be implemented to construct the metallosupramolecular [2×2] grid-type modules $[Fe_4A_4]^{8+}$ (**1**) and $[Fe_4B_4]^{8+}$ (**2**), presenting spin transition behaviour and displaying a collectively generated coordination array, that prepares the structural prerequisites enabling **1** and **2** to undergo a second self-assembly process. This second process leads in both cases to an extended architecture displaying either a one-dimensional columnar $\{\text{-}[Fe_4^{II}A_4]\text{-}(La^{III})\}_n^+$ (**3**), or a two-dimensional wall-like $\{\text{-}[Fe_4^{II}B_4]\text{-}(Ag^I)_4\}_n^{12+}$ (**4**) arrangement. In both higher-order architectures, the magnetic behaviour of the $[Fe_4^{II}L_4]^{8+}$ modules exhibits a progressive hindrance of the spin transition process with increasing dimensionality.

The generation and variation of a certain molecular functionality (here magnetism) at different organisational levels, as realized here in the supramolecular spintronic modules **1/2** and arrays **3/4**, show how the architectural parameters feed-back actively on intrinsic functionalities of complex supramolecular assemblies. It relates to the progressive build-up of functional nanostructured supramolecular devices by sequential self-organization, with concomitant emergence of novel (optical, electronic, magnetic) properties at different levels of system complexity.[1]

Experimental Section

Synthesis of complexes 1 and 2: A solution of ligand **A**[11] (30 mg, 48 μmol) (or **B**[11]) and $[Fe(BF_4)_2] \times 6H_2O$ (16 mg, 48 μmol) in acetonitrile (50 mL) was stirred under reflux for 12 h. Complex **1** (or **2**) was isolated, respectively, as dark green solid by precipitation with diisopropyl ether in quantitative yields (18.0 mg).

The ClO_4 salts of **1** and **2** were synthesized by the same procedure by using $[Fe(ClO_4)_2] \times 6H_2O$. The products obtained exhibit identical spectroscopic properties as the BF_4 salts.

$[Fe_4^{II}A_4](BF_4)_8$ (1): ^1H NMR (200 MHz, CD_3CN, 298 K): $\delta = 118.6$, 62.4, 55.2, 49.9, 47.3, 42.8, 14.5, 7.8, 7.1, 5.6, 4.3, 4.0, 0.7, -7.3; FAB-MS (NBA): m/z: 3132.4 $[M-3BF_4]^+$, 3046.5 $[M-4BF_4]^+$, 2959.6 $[M-5BF_4]^+$, 2871.5 $[M-6BF_4]^+$; UV/Vis (acetonitrile, ε in $10^3 \, cm^2 \, mol^{-1}$): $\lambda = 274$ (189), 365 (41.6), 497 (14.8), 662 nm (15.3); elemental analysis calcd (%) for $C_{160}H_{104}N_{32}B_8Fe_4F_{32} \times 19 H_2O$: C 51.45, H 3.83, N 12.00; found: C 51.47, H 3.36, N 11.70 (for the perchlorate salt $C_{160}H_{104}N_{32}Cl_8Fe_4O_{32} \times 3 CH_3CN \times 4 H_2O$: C 54.05, H 3.31, N 13.29; found: C 54.80, H 3.52, N 13.18.).

$[Fe_4^{II}B_4](BF_4)_8$ (2): ^1H NMR (200 MHz, CD_3CN, 298 K): $\delta = 145.0$, 109.8, 60.4, 52.7, 47.6, 45.9, 41.3, 13.5, 8.1, 4.0, 3.6, 3.5, -1.4, -6.6; FAB-MS (NBA): m/z: 3284.9 $[M-BF_4]^+$, 3219.8 $[M-2BF_4]^+$, 3131.8 $[M-3BF_4]^+$, 3045.8 $[M-4BF_4]^+$, 2958.8 $[M-5BF_4]^+$, 2871.8 $[M-6BF_4]^+$; UV/Vis (acetonitrile, ε in $10^3 \, cm^2 \, mol^{-1}$): $\lambda = 271$ (147), 335 (62.4), 380 (57.0), 496 (9.7), 666 nm (8.7); elemental analysis calcd (%) for $C_{160}H_{104}N_{32}B_8F_{32}Fe_4 \times 6 CH_3CN \times 5 H_2O$: C 55.40, H 3.57, N 14.27; found: C 55.18, H 3.43, N 13.94 (for the perchlorate salt $C_{160}H_{104}N_{32}Cl_8Fe_4O_{28} \times 10 CH_3CN \times 2 H_2O$: C 55.77, H 3.59, N 15.18; found: C 55.40, H 3.63, N 15.11).

Synthesis of assemblies 3 and 4

$\{\text{-}[Fe_4^{II}A_4]\text{-}(La^{III})\}_n(ClO_4)_{(11)n}$ (3): A solution of **1** (as its ClO_4^- salt; 5 mg, 1.43 μmol) in CH_3CN was layered with a solution containing a six-fold excess of $[La(ClO_4)_3]$ (3.8 mg, 8.6 μmol) in methanol (3 mL). After two days, triangle-shaped dark-green prisms of compound **3** were found floating on the solution. An amount of 5.2 mg (1.3 μmol, 92%) of the crystalline material of **3** was collected and directly used in the structural and magnetic investigations. Elemental analysis calcd (%) for $C_{160}H_{104}N_{32}Fe_4LaCl_{11}O_{44} \times 2 CH_3CN \times 16 H_2O$: C 45.79, H 3.33, N 11.07; found: C 44.90, H 3.41, N 10.58.

$\{\text{-}[Fe_4^{II}B_4]\text{-}(Ag^I)_4\}_n(BF_4)_{(12)n}$ (4): A solution of **2** (5 mg, 1.47 μmol) in CH_3CN was layered with a solution of a six-fold excess of $AgBF_4$ (1.8 mg, 8.84 μmol) in methanol (3 mL). After several weeks right-angled pine-green prisms of compound **4** were found at the diffusion interface of the two solutions. An amount of 4.8 mg (1.1 μmol, 75%) of the crystalline material of **4** was collected and directly used in the structural and magnetic investigations. Elemental analysis calcd (%) for $C_{160}H_{104}N_{32}Fe_4Ag_4B_{10}SiF_{46} \times 12 CH_3CN \times 2 H_2O$: C 47.34, H 3.11, N 13.20; found: C 46.95, H 3.22, N 13.01.

Magnetic measurements: They were carried out with a SQUID magnetometer working in the 4.2–300 K temperature range. The applied magnetic field was 1 Tesla. FAB mass spectra were performed on a Fisons TRIO-2000 (Manchester) and a Micromass AUTOSPEC-M-HF spectrometer using 3-nitrobenzylic alcohol as matrix. Microanalyses were carried out by the Service de Microanalyse, Faculté de Chimie, Strasbourg.

X-ray structural analysis of 2 and 4: The data for both compounds were recorded at 120.0(2) K on Beamline ID11 at the European Synchroton Research Facility in Grenoble. Phi rotation images (1 s per frame) were

recorded with a Bruker Smart 6500 camera and a Si(111) monochromated wavelength of 0.45085 Å. The data were integrated with the Bruker data reduction suite Saint and the absorption correction applied via SADABS. Structure solution was performed by direct methods (SHELXS) and refinement against F^2 (SHELXL). The hydrogen atoms were refined with a riding model. As the small size, poor diffracting power of the crystals and volatility of the incorporated solvent molecules led to a low number of strong observations, geometric constraints were applied in order to keep the data/parameter ratio acceptable. The final structures are relatively low resolution and quality, contain disordered counterions and solvent molecules and probably lack further solvent molecules, the positions of which could not be resolved.

The perchlorate salt of **2** was recrystallized by vapour diffusion of benzene into a nitromethane solution of **2** and the obtained green crystals were used in the X-ray investigations.

X-ray structural data for 2: A suitable pine-green prism $(0.02 \times 0.02 \times 0.04$ mm) of **2** $[C_{160}H_{104}N_{32}Fe_4]^{8+} \times 7\,ClO_4 \times Cl^- \times 7\,CH_3NO_2 \times 6\,H_2O$ was obtained from nitromethane/benzene. Complex **2** (at 120 K) monoclinic, $C2/c$, $a = 17.346(2)$, $b = 40.015(6)$, $c = 31.120(4)$ Å, $\beta = 99.150(6)$, $V = 21326(5)$ Å^3, $Z = 4$, $\rho_{calcd} = 1.324$ g cm^{-3}, $2\theta_{max} = 28.36°$, $\mu(Mo_{K\alpha}) = 0.241$ mm^{-1}. 70634 reflections were collected of which 12315 were unique; 10676 of these had $I > 2\sigma(I)$. The final R values were $R = 0.1120$, $wR^2 = 0.2588$ $[I > 2\sigma(I)]$, $R = 0.1271$, $wR^2 = 0.2662$ (all data) for 1348 parameters and 434 restraints. A final difference map displayed the highest electron density of 0.983 e Å^{-3}.

Crystals of **4** were obtained by layering a solution of the BF$_4^-$ salt of **2** in acetonitrile with a solution of methanol containing six equivalents of AgBF$_4$. After several weeks, pine-green prisms of compound **4** had grown at the diffusion interface of the two solutions.

X-ray structural data for 4: Green prisms $(0.01 \times 0.01 \times 0.03$ mm) of $[C_{160}H_{104}N_{32}Fe_4Ag_4]^{12+} \times 10\,BF_4^- \times 1\,SiF_6^{2-} \times 2\,CH_3CN \times 4\,H_2O$ were obtained from acetonitrile/methanol. Complex **4** (at 120 K) monoclinic, $C2/c$, $a = 17.0199(11)$, $b = 43.104(3)$, $c = 30.9306(18)$ Å, $\beta = 99.981(3)$, $V = 22348(2)$ Å^3, $Z = 4$, $\rho_{calcd} = 1.276$ g cm^{-3}, $2\theta_{max} = 24.68°$, $\mu(Mo_{K\alpha}) = 0.365$ mm^{-1}. Of 42249 collected reflections, 11311 were unique and 8279 had $I > 2\sigma(I)$. The final R values were $R = 0.1200$, $wR^2 = 0.2879$ $[I > 2\sigma(I)]$, $R = 0.1528$, $wR^2 = 0.3050$ (all data) for 1470 parameters and 2844 restraints. Although the SiF$_6^{2-}$ anions were not introduced initially, they probably form by reaction with the glass container when BF$_4^-$ ions are present and are incorporated in the crystals. This is not uncommon (see for instance ref. [10]).

CCDC-238750 (**2**) and -238751 (**4**) contain the supplementary crystallographic data for this paper. These data can be obtained free of charge via www.ccdc.cam.ac.uk/conts/retrieving.html, or from the Cambridge Crystallographic Data Centre, 12 Union Road, Cambridge CB2 1EZ, UK; fax: (+44)1223-336033; or email: deposit@ccdc.cam.ac.uk.

Acknowledgement

[1] a) J.-M. Lehn, *Proc. Natl. Acad. Sci. USA* **2002**, *99*, 4763–4768; b) J.-M. Lehn, *Science* **2002**, *295*, 2400–2403; c) J.-M. Lehn, *Supramolecular Chemistry. Concepts and Perspectives*, Vch, Weinheim, **1995**, pp. 139–197 and pp. 201–203.

[2] D. Philp, J. F. Stoddart, *Angew. Chem.* **1996**, *108*, 1242–1286; *Angew. Chem. Int. Ed.* **1996**, *35*, 1154–1196.

[3] S. Oliver, N. Coombs, A. Kuperman, A. Lough, G. A. Ozin, *Nature* **1995**, *378*, 47–50; S. Oliver, N. Coombs, G. A. Ozin, *Adv. Mater.* **1995**, *7*, 931–935; J. A. Real, E. Andrés, M. C. Munoz, M. Julve, T.

Granier, A. Bousseksou, F. Varret, *Science* **1995**, *268*, 265–268; D. Walsh, S. Mann, *Nature* **1995**, *377*, 320–323; C. T. Kresge, *Adv. Mater.* **1996**, *8*, 181–182; V. G. Machado, A. S. Mangrich, J.-M. Lehn, *J. Braz. Chem. Soc.* **2003**, *14*, 777–789.

[4] Illustrations from our own work involve the three level self-organization processes of two complementary monomers into supramolecular polymeric chains that assemble into triple helical filaments: a) C. Fouquey, J.-M. Lehn, A.-M. Levelut, *Adv. Mater.* **1990**, *2*, 254–257; T. Gulik-Krczywicki, C. Fouquey, J.-M. Lehn, *Proc. Natl. Acad. Sci. USA* **1993**, *90*, 163–164, and of three sector shaped molecules into supramolecular disks that stock to form a column: b) D. Suarez, J.-M. Lehn, S. C. Zimmermann, A. Skoulios, B. Heinrich, *J. Am. Chem. Soc.* **1998**, *120*, 9526–9532; in both cases these two steps are followed by association of the two objects formed into a supramolecular liquid crystalline phase; see also c) J.-M. Lehn, *Polym. Int.* **2002**, *51*, 825–839.

[5] C. Kuehl, T. Yamamoto, S. R. Seidel, P. J. Stang, *Org. Lett.* **2002**, *4*, 913–915; B. J. Holliday, C. A. Mirkin, *Angew. Chem.* **2001**, *113*, 2076–2097; *Angew. Chem. Int. Ed.* **2001**, *40*, 2022–2053; G. F. Swiegers, T. J. Malefetse, *Chem. Rev.* **2000**, *100*, 3483–3537; S. Leiniger, B. Olenyuk, P. J. Stang, *Chem. Rev.* **2000**, *100*, 853–878; S. Leininger, J. Fan, M. Schmitz, P. J. Stang, *Proc. Nat. Acad. Sci. USA* **2000**, *97*, 1380–1384; P. N. W. Baxter, J.-M. Lehn, G. Baum, D. Fenske, *Chem. Eur. J.* **1999**, *5*, 102–105; N. Takeda, K. Umemoto, K. Yamaguchi, M. Fujita, *Nature* **1999**, *398*, 794–796; B. Olenyuk, J. A. Whiteford, A. Fechtenkötter, P. J. Stang, *Nature* **1999**, *398*, 796–799; M. Fujita, *Chem. Soc. Res.* **1998**, *6*, 417–433; S. R. Seidel, P. J. Stang, *Acc. Chem. Res.* **2002**, *35*, 972–983; D. L. Caulder, K. N. Raymond, *Acc. Chem. Res.* **1999**, *32*, 975–991; P. J. Stang, B. Olenyuk, *Acc. Chem. Res.* **1997**, *30*, 502–518; P. N. W: Baxter, in *Comprehensive Supramolecular Chemistry, Vol. 9* (Eds.: J. L. Atwood, J. E. D. Davies, D. D. MacNicol, F. Vögtle, J.-M. Lehn), Pergamon, Oxford **1996**, Chapter 5, 165–211.

[6] For some selected examples: J.-P. Collin, C. O. Dietrich Buchecker, P. Gavina, M. C. Jiminez-Molero, J.-P. Sauvage, *Acc. Chem. Res.* **2001**, *34*, 477–487; V. Balzani, A. Credi, F. M. Raymo, J. F. Stoddart, *Angew. Chem.* **2000**, *112*, 3484–3530; *Angew. Chem. Int. Ed.* **2000**, *39*, 3348–3391; C. P. Collier, G. Mattersteig, E. W. Wong, Y. Luo, K. Beverly, F. M. Raymo, J. F. Stoddart, J. R. Heath, *Science* **2000**, *289*, 1172–1176; C. P. Collier, G. Mattersteig, E. W. Wong, Y. Luo, J. Sampaio, F. M. Raymo, J. M. Stoddart, J. R. Health, *Science* **1999**, *285*, 391–395; J.-P. Sauvage, *Acc. Chem. Res.* **1998**, *31*, 611–619; R. Ballardini, V. Balzani, M. T. Gandolfini, L. Prodi, M. Venturi, D. Philp, H. G. Ricketts, J. F. Stoddart, *Angew. Chem.* **1993**, *105*, 1362–1365; *Angew. Chem. Int. Ed. Engl.* **1993**, *32*, 1301–1303.

[7] As a biological example, the light-harvesting function of the Mg-porphyrins within the photosynthetic antenna systems is modular and the photophysical properties of the units are altered and directed by the formation of supramolecular assemblies: see P. Jourdan, P. Fromme, H. T. Witt, O. Klukas, W. Saenger, N. Krauß, *Nature* **2001**, *411*, 909–917.

[8] Electrochemical: a) M. Ruben, E. Breuning, J.-P. Gisselbrecht, J.-M. Lehn, *Angew. Chem.* **2000**, *112*, 4312–4315; *Angew. Chem. Int. Ed.* **2000**, *39*, 4139–4142; M. Ruben, E. Breuning, M. Barboiu, J.-P. Gisselbrecht, J.-M. Lehn, *Chem. Eur. J.* **2003**, *9*, 291–299; b) magnetic: O. Waldmann, J. Hassmann, P. Müller, G. S. Hanan, D. Volkmer, U. S. Schubert, J.-M. Lehn, *Phys. Rev. Lett.* **1997**, *78*, 3390–3393; c) optical: M. Ruben, J.-M. Lehn, G. Vaughan, *Chem. Commun.* **2003**, 1338–1339.

[9] a) E. Breuning, M. Ruben, J.-M. Lehn, F. Renz, Y. Garcia, V. Ksenofontov, P. Gütlich, E. Wegelius, K. Rissanen, *Angew. Chem.* **2000**, *112*, 4312–4315; *Angew. Chem. Int. Ed.* **2000**, *39*, 2504–2507; b) M. Ruben, E. Breuning, J.-M. Lehn, V. Ksenofontov, F. Renz, P. Gütlich, G. Vaughan, *Chem. Eur. J.* **2003**, *9*, 4422–4429 and corrigendum, *Chem. Eur. J.* **2003**, *9*, 5176; c) M. Ruben, E. Breuning, J.-M. Lehn, V. Ksenofontov, P. Gütlich, G. Vaughan, *J. Magn. Magn. Mater.* **2004**, *272–276*, e715–e717.

[10] E. Breuning, U. Ziener, J.-M. Lehn, E. Wegelius, K. Rissanen, *Chem. Eur. J.* **2001**, *7*, 1515–1521.

[11] U. Ziener, J.-M. Lehn, A. Mourran, M. Möller, *Chem. Eur. J.* **2002**, *8*, 951–957.

[12] I. Bertini, C. Luchinat, " *NMR of Paramagnetic Molecules in Biological Systems*", 1st ed., Benjamin/Cummings Publishing Company, Amsterdam, Sydney, **1986**.

[13] R. L. Carlin, " *Magnetochemistry*", 1st ed., Springer, Berlin, **1986**.

[14] O. Kahn, C. J. Martinez, *Science* **1998**, *279*, 44–48; P. Gütlich, A. Hauser, H. Spiering, *Angew. Chem.* **1994**, *106*, 2109–2141; *Angew. Chem. Int. Ed. Engl.* **1994**, *33*, 2024–2054; and references therein.

For a recent text on spin crossover in transition-metal compounds, see: *Top. Curr. Chem. Vol. 233* (Eds.: P. Gütlich, H. A. Goodwin), Springer, **2004**.

[15] E. König, *Nature and Dynamics of the Spin-State Interconversion in Metal Complexes*, *Vol. 76*, Springer, Berlin, Heidelberg, **1991**.